The Hosts of Megamaser Disk Galaxies (II)

Scientific Category:	AGN/QUASARS
Scientific Keywords:	Galaxy Centers, Host Galaxies, Seyfert Galaxies
Instruments:	WFC3

Proprietary Period: 12

Orbit Request	Prime	Parallel
Cycle 22	20	0

Abstract

We propose to observe ten new megamaser disk galaxies. Much like in NGC 4258, the megamasers in our sample trace sub-pc, circumnuclear gas in Keplerian rotation around central supermassive black holes (BHs). From the maser disk, we derive the most precise BH masses (<10%) outside of our own Galactic Center, as well as a very precise orientation for the megamaser disk. These megamaser galaxies are the best available tool to study BH demographics in spiral galaxies, but HST resolution is required to disentangle the nuclear disks, star-forming rings, bars, and dust from any underlying bulge component. Using F336W, F438W, F814W, F110W, and F160W observations of these galaxies with WFC3, we will derive accurate bulge masses to study BH-galaxy scaling relations. We will then compare the orientation of the ~100 pc-scale structures we find with that of the accretion disk on sub-pc scales, to determine the mechanisms that connect the galactic ISM to accretion. The ten new megamaser disk systems proposed here not only double the entire megamaser sample with uniform HST imaging, but crucially add six new dynamical BH masses with $M\_BH < 10^7$ M_sun.

Investigators:

	Investigator	Institution	Country
PI&	J Greene	Princeton University	USA/NJ
CoI	A Seth	University of Utah	USA/UT
CoI*	R Laesker	Max-Planck-Institut fur Astronomie, Heidelberg	DEU
CoI	J Braatz	Associated Universities, Inc.	USA/VA
CoI	F Lo	National Radio Astronomical Observatory	USA/WV
CoI*	C Henkel	Max-Planck-Institut fur Radioastronomie	DEU

Number of investigators: 6

* ESA investigators: 2

& Phase I contacts: 1

Target Summary:

Target	RA	Dec	Magnitude
NGC-449	01 16 7.2280	+33 05 21.80	V = 15.0
MRK-1029	02 17 3.5740	+05 17 31.02	V = 15.8
J0437+2456	04 37 3.6900	+24 56 7.00	V = 16.6
UGC-3193	04 52 52.5860	+03 03 25.90	V = 14.8
ESO-558-9	07 04 21.0020	-21 35 19.36	V = 15.8
MRK-1210	08 04 5.8410	+05 06 49.84	V = 14.3
UGC-6093	11 00 47.9550	+10 43 41.76	V = 14.8
NGC-5495	14 12 23.3530	-27 06 28.72	V = 13.5
NGC-5728	14 42 23.9280	-17 15 11.41	V = 13.4
MCG+01-38-005	14 50 51.5110	+05 06 52.20	V = 14.5

Observing Summary:

Target	Config Mode and Spectral Elements	Flags	Orbits
NGC-449	WFC3/IR Imaging F110W		2
	WFC3/IR Imaging F160W		
	WFC3/UVIS Imaging F336W		
	WFC3/UVIS Imaging F438W		
	WFC3/UVIS Imaging F814W		
MRK-1029	WFC3/IR Imaging F110W		2
	WFC3/IR Imaging F160W		

Target	Config Mode and Spectral Elements	Flags	Orbits
	WFC3/UVIS Imaging F336W		
	WFC3/UVIS Imaging F438W		
	WFC3/UVIS Imaging F814W		
J0437+2456	WFC3/IR Imaging F110W		2
	WFC3/IR Imaging F160W		
	WFC3/UVIS Imaging F336W		
	WFC3/UVIS Imaging F438W		
	WFC3/UVIS Imaging F814W		
UGC-3193	WFC3/IR Imaging F110W		2
	WFC3/IR Imaging F160W		
	WFC3/UVIS Imaging F336W		
	WFC3/UVIS Imaging F438W		
	WFC3/UVIS Imaging F814W		
ESO-558-9	WFC3/IR Imaging F110W		2
	WFC3/IR Imaging F160W		
	WFC3/UVIS Imaging F336W		
	WFC3/UVIS Imaging F438W		
	WFC3/UVIS Imaging F814W		
MRK-1210	WFC3/IR Imaging F110W		2
	WFC3/IR Imaging F160W		
	WFC3/UVIS Imaging F336W		
	WFC3/UVIS Imaging F438W		
	WFC3/UVIS Imaging F814W		
UGC-6093	WFC3/IR Imaging F110W		2
	WFC3/IR Imaging F160W		
	WFC3/UVIS Imaging F336W		
	WFC3/UVIS Imaging F438W		
	WFC3/UVIS Imaging F814W		
NGC-5495	WFC3/IR Imaging F110W		2
	WFC3/IR Imaging F160W		
	WFC3/UVIS Imaging F336W		
	WFC3/UVIS Imaging F438W		
	WFC3/UVIS Imaging F814W		
NGC-5728	WFC3/IR Imaging F110W		2
	WFC3/IR Imaging F160W		
	WFC3/UVIS Imaging F336W		
	WFC3/UVIS Imaging F438W		
	WFC3/UVIS Imaging F814W		
MCG+01-38-005	WFC3/IR Imaging F110W		2
	WFC3/IR Imaging F160W		
	WFC3/UVIS Imaging F336W		

Target	Config Mode and Spectral Elements	Flags	Orbits
	WFC3/UVIS Imaging F438W		
	WFC3/UVIS Imaging F814W		

Total prime orbits: 20

■ Scientific Justification

1 Megamaser-Disk Galaxies: A Key to Black Hole Demographics

The galaxy NGC 4258 contains a remarkable megamaser at its center. This circumnuclear megamaser traces Keplerian rotation around the supermassive black hole (BH) at a radius of ~ 0.2 pc (Miyoshi et al. 1995) and modeling of the maser emission yields the most precise supermassive BH mass measurement apart from our own Galactic Center (e.g., Herrnstein et al. 1999). In fact, the deviations from Keplerian rotation are so small that it is possible to rule out most astrophysically plausible alternatives to a supermassive BH in the center of this galaxy (e.g., Maoz 1998). Furthermore, by tracing the accelerations of individual spots, it is possible to derive an angular diameter distance to NGC 4258 (e.g., Herrnstein et al. 1999), which has also been used to calibrate Cepheid distances (Riess et al. 2011; Humphreys et al. 2013).

Recently, sensitive surveys enabled primarily by the Green Bank Telescope (GBT) have revealed many new megamaser disks (e.g., Braatz and Gugliucci 2008; Reid et al. 2009; Greenhill et al. 2009; Fig. 1). The galaxies are composed of $\sim L^*$ spiral galaxies with Hubble types S0-Sbc, while the derived BH masses have values near $M_{\rm BH} \sim 10^7 \ M_\odot$. *These maser galaxies are by far the best tools for probing BH demographics in spiral galaxies, and have already shown definitively that the M-sigma relationship defined for early type galaxies does not hold in these systems (Greene et al. 2010).* In this proposal we build on our successful Cycle 18 proposal, and focus on **ten** new megamaser disk galaxies with VLBA imaging in hand, for which we can determine both a BH mass to better than $< 10\%$ and the orientation of the megamaser disk. Six of the galaxies in our sample have BH masses $M_{\rm BH} < 10^7 \ M_\odot$, bringing the total number in this mass range from 8 to 14 (McConnell & Ma 2013), including four new systems with $M_{\rm BH} < 5 \times 10^6 \ M_\odot$.

Megamaser disk galaxies have redefined our understanding of BH demographics and active galactic nucleus (AGN) fueling. We have leveraged the precise BH masses to study the scaling relations between BH mass and σ_* (Greene et al. 2010), bulge luminosity and mass (Läsker et al. in preparation; Figure 2), and halo mass (Sun et al. 2013). We have a pending VLT/SINFONI program to obtain a stellar dynamical BH mass measurement for NGC 4388, to provide an invaluable check against the megamaser-disk mass (e.g., Siopis et al. 2009). Only *HST* imaging can allow us to approach the scale of the BH sphere of influence with optical imaging to study fueling mechanisms in the galaxy nuclei (Greene et al. 2013, 2014), which strongly complements observations of cold gas kinematics facilitated by ALMA (already underway for the nearest systems; PI Henkel). We have shown (Greene et al. 2013) that in order to disentangle stellar population variations, extinction, narrow-line emission, and hot dust from the AGN, we require multi-band imaging on < 100pc scales that only *HST* can provide.

2 Why *HST*? The Delightful Complexity of Spiral Galaxy Nuclei

Our *HST* imaging of the megamaser disk galaxies observed to date has revealed a rich and complicated phenomenology. On < 500 pc scales, we see some combination of bars, rings, and spirals in the center of every galaxy in our sample (Läsker et al. in prep; Figure 2). We simply cannot understand the complicated relationship between BHs and spiral galaxies without *HST* imaging. Without the spatial resolution of *HST*, we will confuse light from the larger and typically rounder bulge component with the light from blue and centrally concentrated, kinematically cold structures. This decomposition is critical to fully study galaxy scaling relations. Note that both the stellar velocity dispersion σ_* and the bulge mass are prone to confusion from such structures. At the same time, we gain new insight into the fueling mechanisms of these active galaxies by studying the kinematically cold and non-axisymmetric structures that drive secular evolution on these small scales. For the targets in our sample, 200 pc ranges from $0\rlap{.}{''}3$ to $1\rlap{.}{''}25$, with a median size of $0\rlap{.}{''}4$. If we are to reliably identify these nuclear structures, we require *HST*. Multi-band WFC3 data ranging from the UV through the NIR will allow us to address the following two key problems in BH demographics.

Do spiral galaxies obey any galaxy-BH scaling relations? Over the last fifteen years, we have come to believe that accretion energy from supermassive BHs plays a central role in galaxy evolution (e.g., Hopkins et al. 2006), leading to the tight observed scaling relations between central supermassive BHs and the properties of their surrounding galaxies (e.g., McConnell & Ma 2013). However, prior to the discovery of large new samples of megamaser disk galaxies there were only a handful of dynamical BH measurements in spiral galaxies. Using the megamaser disk galaxies, we showed that there is no correlation between central BH mass and σ_* in $\sim L^*$ spiral galaxies (Greene et al. 2010); adding the new sample significantly strengthens this conclusion by extending the sample to even lower mass BHs (Figure 3; Greene et al. in prep).

Interpreting the observed lack of correlation, however, is quite challenging. Perhaps it tells us that spiral galaxies, and their BHs, grow in a fundamentally different way from elliptical galaxies (e.g., Kormendy & Ho 2013). Or perhaps σ_* is a red herring. Unlike in elliptical galaxies, kinematically cold structures at arbitrary inclinations are to be found behind varying levels of dust extinction, yielding complicated two-dimensional dispersion profiles that often fall towards the center (e.g., Peletier et al. 2007; Greene et al. 2014). We must investigate whether there are cleaner probes of BH-galaxy correlations in spiral galaxies. Specifically, can we look through the dust and young stars to find a true bulge in these galaxies, and does the mass of that bulge component correlate with $M_{\rm BH}$? Based on our current sample, Läsker et al. in prep. find that $M_{\rm bulge}$ may correlate more tightly with $M_{\rm BH}$ than σ_* (Figure 3). However, the existing sample is still quite small; of the ten targets in this proposal, six have $M_{\rm BH} < 10^7 \ M_\odot$, allowing us to examine scatter in the $M_{\rm BH}$-$L_{\rm bulge}$ relation as a function of $M_{\rm BH}$ in this low-mass regime for the first time.

What drives the fueling of moderate luminosity active galaxies? The fueling mechanisms of growing BHs are likely to be intimately related to the final BH-galaxy scaling
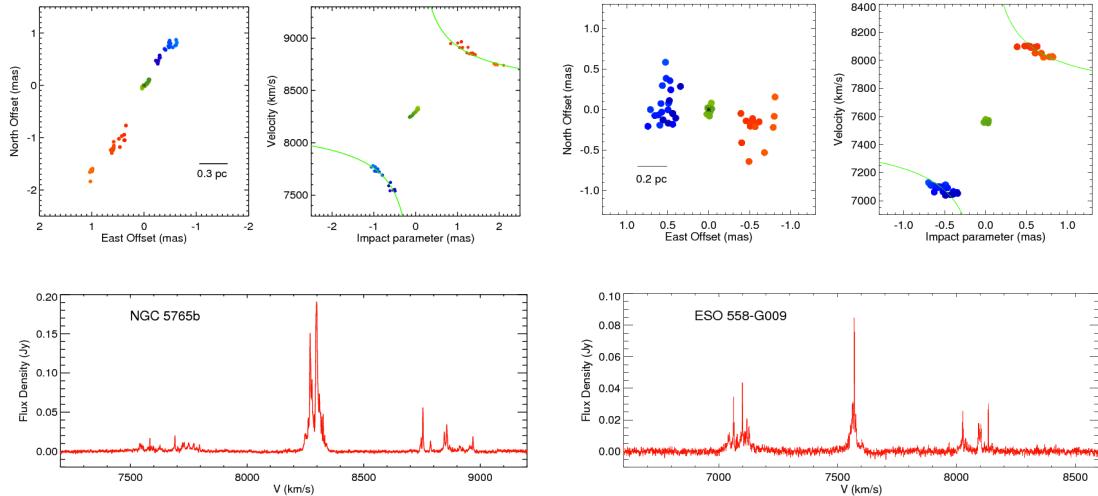
relations. Rather than a dramatic, merger-induced quasar episode, perhaps these lower-mass BHs are fed by small dribbles of gas supplied by secular transport via spiral arms, bars, and nuclear disks (e.g., Kormendy & Kennicutt 2004). This "secular" mode is apparently the dominant mode of BH growth even at the peak of quasar activity, $z \approx 2$ (e.g., Schawinski et al 2011; Cisternas et al. 2011; Kocevski et al. 2012). The megamaser disk galaxies provide a unique opportunity to study secular growth in detail because *we know the orientation of the accretion disk on sub-pc scales extremely precisely.* Thanks to *HST*, we can identify the signatures of secular evolution in the galaxy nuclei, and measure their projected orientation. The surprising result from our Cycle 18 program is that even on ~ 200 pc scales, there is no correlation between the orientation of the cold nuclear structures and that of the maser disk (Greene et al. 2013). Such a change in angular momentum is predicted if torques between stars and gas on multiple scales ultimately fuels the BH (e.g., Hopkins & Quataert 2010). *We propose here to observe ten additional galaxies, which doubles the number of galaxies in our analysis.*
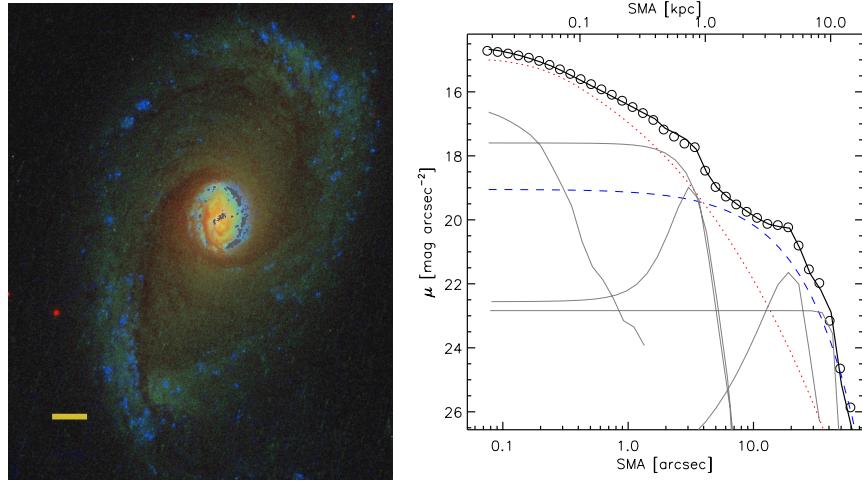
3 Proposed *HST* Program and Scientific Objectives

To jointly constrain variations in stellar populations, dust extinction, and possible AGN emission at long wavelengths, we propose to obtain WFC3 imaging in F336W, F438W, F814W, F110W and F160W for each galaxy. In combination with deep ground-based imaging, we will perform multi-band, two-dimensional decompositions using the program GALFIT (Peng et al. 2002, 2010; Fig. 4). Adding ten new galaxies with uniform imaging, for a total sample of 19 galaxies, we will:

• Identify the true "bulge" component of the galaxy, free from contamination by components like bars and rings, and correcting for dust extinction. Determine host galaxy morphologies. Use the multi-color photometry to fit stellar population models and thus determine a stellar mass as well as luminosity for the bulge component. Evaluate whether these galaxies obey BH-bulge scaling relations.

• Using radial profiles, colors, and two-dimensional fitting to identify nuclear bars, spirals, and rings. Compare the PA of these components with the precisely known maser disk orientation, to ask whether statistically the angular momentum of gas changes, and by how much, as it accretes into the final 200 pc. With 20 targets we will have the statistics to look for trends as a function of the bulge-to-total ratio, as predicted by Hopkins & Quataert.

• Use the five-band imaging to identify pixels that are dominated by narrow emission lines (Greene et al. 2013) and look for radio-entrained gas by matching with our ongoing JVLA program (PI Henkel).

• Look for a red, unresolved nuclear source in the F160W image that would be the signature of hot dust from the active nucleus (e.g., Quillen et al. 2001). Use this luminosity as an additional bolometric luminosity indicator for the active nucleus.
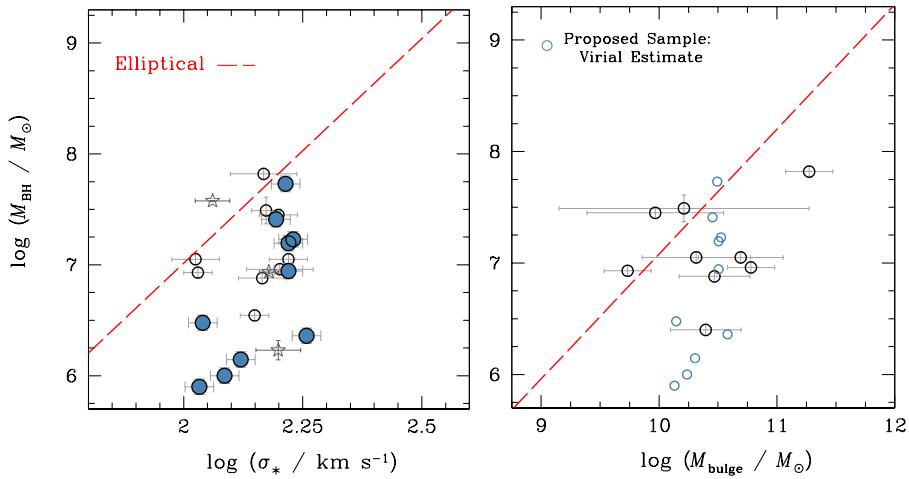
References Braatz, J. A., & Gugliucci, N. E. 2008, ApJ, 678, 96; Cisternas, M., et al. 2011, ApJ, 726, 57; Greene, J. E., et al. 2014, submitted; Greene, J. E., Seth, A., den Brok, M., et al. 2013, ApJ, 771, 121; Greene, J. E., Peng, C. Y., Kim, M., et al. 2010, ApJ, 721, 26; Greene, J. E., et al. 2008, ApJ, 688, 159; Greenhill, L. J., et al. 2009, ApJ, 707, 787; Häring, N., & Rix, H.-W. 2004, ApJL, 604, L89; Herrnstein, J. R., et al. 1999, Nature, 400, 539; Hopkins, P. F., et al. 2006, ApJS, 163, 1; Hopkins, P. F., & Quataert, E. 2010, MNRAS, 407, 1529 ; Humphreys, E. M. L., et al. 2013, ApJ, 775, 13; Kormendy, J., & Ho, L. C. 2013, ARA&A, 51, 511; Kormendy, J., & Kennicutt, R. C., Jr. 2004, ARA&A, 42, 603; Läsker, R., et al. 2014, ApJ, 780, 70; Maoz, E. 1998, ApJ, 494, L181; Miyoshi, M., et al. 1995, Nature, 373, 127; McConnell, N. J., & Ma, C.-P. 2013, ApJ, 764, 184; Peletier, R. F., et al. 2007, MNRAS, 379, 445; Peng, C. Y., et al. 2002, AJ, 124, 266; Peng, C. Y., et al. 2010, ApJ, 139, 2097; Quillen, A. C., et al. 2001, ApJ, 547, 129; Reid, M. J., et al. 2009, ApJ, 695, 287; Riess, A. G., et al. 2011, ApJ, 730, 119; Siopis, C., et al. 2009, ApJ, 693, 946; Sun, A.-L., Greene, J. E., et al. 2013, ApJ, 778, 47; Zibetti, S., et al. 2009, MNRAS, 400, 1181

Figure 1 — Two of the new megamaser disk galaxies in the proposed sample. For each system we show the megamaser spatial distribution (*top left*) and rotation curve (*top right*) and spectrum (*bottom*) (Gao et al. in prep). Color corresponds to velocity, with bluer/redder spots having higher velocities towards/away from us respectively. The linear distribution of maser spots on the sky strongly implicates a disk orientation within 2°of edge-on, meaning that the BH mass uncertainties ($\sim 10\%$) are dominated by the uncertainty in distance to the galaxy.

Figure 2 — Left: Image of UGC 3789 using our three WFC3/UVIS bands (F336W, F435W, F814W). The scale bar indicates $4''$ (1 kpc). North is up and East to the left. The two prominent star-forming rings are easily seen in the radial profile as well. Note the complex nuclear structures, including a bar and ring, on sub-arcsec scales. *Right*: Radial profile of the galaxy in F160W (open circles) and best-fit GALFIT model (solid) broken into components, with the bulge shown in dotted red and the disk in dashed blue (Läsker et al. in prep). We also identify an inner flattened component.

Figure 3 — Left: The lack of correlation between M_{BH} and σ_* for megamaser disk galaxies. Stellar velocity dispersions are measured in $2''$ radii, with no contamination from the kpc-scale disk. Blue symbols are the galaxies proposed for here (Greene et al. in prep) while open circles are from Greene et al. (2010) and stars and red-dashed line are from McConnell & Ma (2013). *Right*: Relationship between bulge mass and M_{BH} for the galaxies in our Cycle 18 *HST* proposal (black open circles; Läsker et al. in prep). The bulge luminosity is determined from GALFIT models to the F160W data, while the mass-to-light ratio uses bulge colors from the optical bands and the conversion of Zibetti et al. (2009). In blue, we show where the new sample may fall assuming that $M_{\mathrm{bulge}} \propto \sigma^2 r$;

5

the new sample is crucial to extend our sample below $M_{\rm BH} \lesssim 10^7\ M_\odot$. The elliptical galaxy relation is taken from Häring & Rix (2004). Our data may suggest that bulge luminosity correlates more strongly with $M_{\rm BH}$ than σ_*. By doubling the sample as proposed here, we will be able to address the scatter in the relation as a function of mass, as well as sub-divide the sample by morphological type.

Description of the Observations

Table 1.   The Sample

Galaxy	RA	Dec.	D	Hubble Type	m_B	Size	Inc
(1)	(2)	(3)	(4)	(5)	(6)	(7)	(8)
NGC449	01:16:07.2	33:05:22	68	SBa	15.0	0.68	61
Mrk1029	02:17:03.5	05:17:31	124	S	15.8	0.59	46
J0437+2456	04:37:03.7	24:56:07	66	S	16.6	$\cdots$	17
UGC3193	04:52:52.6	03:03:26	64	SBb	14.8	0.92	76
ESO558-G009	07:04:21.0	-21:35:19	103	Sbc	15.8	1.15	81
Mrk1210	08:04:05.8	05:06:50	58	Sa	14.3	0.85	16
UGC6093	11:00:47.9	10:43:41	150	SBbc	14.8	1.19	38
NGC5495	14:12:23.3	-27:06:29	93	SBc	13.5	1.52	35
NGC5728	14:42:23.9	-17:15:11	32	SBa	14.5	3.16	59
MCG+01-38-005	14:50:51.5	05:06:52	113	SABb	14.5	0.81	49

Note. — Col. (1): Name. Col. (2): Right Ascension (hrs; J2000). Col. (3): Declination (deg; J2000). Col. (4): Distance (Mpc). Col. (5): Hubble type from RC3 (de Vaucouleurs et al. 1992) as compiled in NED. Col. (6): Apparent magnitude (B_T; mag) from RC3. Col. (7): Approximate galaxy size from NED ($'$). Col. (8): Galaxy inclination (degrees).

We take as our sample the ten new megamaser disk galaxies with VLBI mapping in hand, for which we can derive $M_{\rm BH}$ and a disk orientation, both required for the science proposed here (Table 1). With distances of $18 - 150$ Mpc, the galaxies have apparent magnitudes of $m_B = 15.4 - 12.5$ mag and apparent sizes ranging from $\sim 0.5 - 3'$ (~ 15 kpc at 50 Mpc). *Combined with our successful Cycle 18 program, this proposal will provide observations of 19 megamaser disk galaxies with uniform depth and filter coverage.*

Choice of Filters and Camera: Our observational strategy is identical to that of our Cycle 18 program. In order to disentangle, both spectrally and spatially, variations in stellar populations, dust absorption, and dust emission from the AGN, we require multiple filters. In the UV we take F336W (broad U), which allows us to probe the near UV part of the spectrum with reasonable throughput, while in the blue we choose F438W to avoid contamination from Hβ emission. In the red we take F814W (broad I) because of its high throughput and to avoid contamination from emission lines such as [O III] $\lambda 5007$. In the near-infrared, from our fits we find some contamination from dust heated by the active galaxy continuum in the F160W filter, while galaxy light dominates the F110W filter (e.g., Alonso-Herraro et al. 1996). We thus request both F110W and F160W to ensure that we have a NIR AGN-free filter. WFC3 is the camera of choice, as it will allow us to cover the entire wavelength range

with the highest sensitivity and finest pixel scale.

Observational Plan. To robustly decompose any round bulge component from disks, bars, and rings, we seek sensitivity to $\mu_V \sim 22$ mag arcsec^{-2} at $\sim 5 - 10''$, which is typically a factor of a few below the total surface brightness at these scales (Fig. 2). Secondly, because we are interested in decoupling various non-axisymmetric components, such as bars, and to facilitate combining with ground-based data, we require S/N> 5 at $\sim 20''$ scales (as faint as $\mu_V \sim 24.5$ mag arcsec^{-2}; Fig. 3) in our deepest filters (IH). These goals can be accomplished in two ~ 51 min orbits per galaxy. In the UVIS, we will use a three-point dither pattern to facilitate cosmic-ray and hot-pixel removal. In the IR, we will use the WFC3-IR-DITHER-BOX in order to properly sample the PSF. For filters with short exposures (F438W, F110W, F160W) we will use subarrays (2k×2k and IRSUB512 respectively) to avoid buffer dumps.

In summary, the exposure times for each filter are as follows:

• F336W: for nuclear disks and bulge stellar populations, require S/N> 50 in the nucleus; 3×400 sec.

• F438W: the same as F336W; 3×130 sec.

• F814W: for galaxy structural measurements, requires S/N> 5 at $\mu_V = 24.5$ mag arcsec^{-2}; 3×640 sec.

• F110W: for stellar populations, dust, and structural measurements, requires S/N> 5 at $\mu_V = 24.5$ mag arcsec^{-2}; 4×30 sec.

• F160W: combination of AGN and nuclear star cluster at the center, also our deep near-infrared structural image; requires 4×100 sec.

We divide the exposures as follows, based on our successful Cycle 18 program. Orbit 1 will proceed as F110W (4×30 sec)-F438W (1×130 sec)-F336W (3×400 sec)-F438W (2×130 sec). Since the first two filters use subarrays, we incur no buffer dumps, but spend 22 min on overheads (6 for guide-star acquisition, 12.4 min for readout, 2.5 min for dithering, and 1 min to change from IR to UVIS). Orbit 2 will be the remaining filters: F160W (4×100 sec)-F814W (3×690 sec). The long exposures in F814W allow us to read out the full array with no buffer dumps. In some of the brightest/nearest galaxies we may saturate in the three redder filters. Our readout modes (STEP25, with NSAMP=5 for F110W and NSAMP=8 for F180W) and dithering should mitigate this problem and possible persistence in the IR channel, while in F814W we will take an additional short exposure where required. We note that there is some danger for a low-level jump in the background level for the F110W and F160W observations, which will hopefully be removed in software, but should not significantly impact the observations of these bright galaxies.

We request a total of 20 orbits to image the entire sample.

Analysis Plan.

We will perform 2-D image analysis to decompose the megamaser galaxies using the updated version of GALFIT 3.0 (Peng et al. 2010) that has been broadly used to analyze *HST* images of normal as well as active galaxies. GALFIT 3.0 can fit spiral arms and non-axisymmetric components, which is required for decomposition of bulge components and searching for star clusters in these complex nuclear regions (Fig. 4). For galaxies whose apparent sizes are larger than the *HST* images, we will make use of structural parameters

of the extended disk (e.g. size, luminosity and axis ratio) derived from ground-based images taken using the du Pont, APO 3.5m, and WIYN telescopes. These images have been taken and analyzed, and Läsker et al. in prep. have developed a robust method to combine the ground-based and space-based images for combined fitting that accounts for zero-point, background, pixel-scale, and PSF differences.

Auxiliary Data.

 Data acquisition in progress:
- Long-slit spectroscopy for all with S/N> 30 per pixel (Greene et al. in prep).
- $UVRIK$ imaging for nearly all galaxies is complete.

 Data we plan to acquire:
- AO-assisted NIR IFU spectroscopy for the Southern targets with VLT/SINFONI+AO.
- HI rotation curves.
- Ongoing programs have obtained ALMA data for a handful of the nearest megamaser disk galaxies (NGC 1068, Circinus, NGC 4945) and PI Greene has applied for ALMA CO (6-5) and CO (3-2) observations of one megamaser disk galaxy (NGC 4388). Eventually as the array grows we plan to target more of these systems.

■ Special Requirements

None.

■ Coordinated Observations

None.

■ Justify Duplications

Three galaxies in our sample have existing archival *HST* imaging, Mrk 1, Mrk 1210, and NGC 5728. For NGC 5728 there is only UV imaging, which we will use to augment our observations but do not achieve our science goals. Mrk 1 has no NIR data, and only very short exposures in F547M, F606W and F814W, while Mrk 1210 has only a short F606W and F160W exposure. Thus, the existing data are not adequate to meet our needs, and we request the full data set for all galaxies.

■ Past HST Usage and Current Commitments

PI Greene is involved in the following programs:
- GO-12185 (PI: Jenny Greene). Observations completed, and analysis published in Greene et al. 2013, ApJ, 771, 121; Greene et al. 2014, ApJ, submitted; Läsker et al. in preparation.
- GO-12745 (PI: Julia Comerford). Observations completed and analysis underway at U of Colorado.
- GO-12163 (PI: Aaron Barth). Observations completed and analysis underway at UC Irvine.

- GO-11662 (PI: Misty Bentz). Observations completed and published: Bentz, M. C., et al. 2013, ApJ, 767, 149
- GO-11130 (PI: Luis Ho). Observations completed and published: Jiang, Y.-F., Greene, J. E., et al. 2011, ApJ, 742, 68; Jiang, Y.-F., Greene, J. E., & Ho, L. C. 2011, ApJL, 737, L45
- GO-10596 (PI: Luis Ho). Results published: Greene et al. 2008, ApJ 688, 159.